

## PHASE CHANGE AND THERMOCHROMISM OF CRYSTALLINE 2,4-DIHYDROXYBENZYLIDENE-4-AMINOANTIPYRINE AND ITS $\text{UO}_2(\text{VI})$ COMPLEX IN THE SOLID STATE

F.A. EL-SAIED <sup>a,\*</sup>, M.M. AYAD <sup>b</sup> and M.I. AYAD <sup>a</sup>

<sup>a</sup> *Department of Chemistry, Faculty of Science, El-Menoufia University, Shebin El-Kom (Egypt)*

<sup>b</sup> *Department of Chemistry, Faculty of Science, Tanta University, Tanta (Egypt)*

(Received 5 December 1989; in final form 31 January 1990)

### ABSTRACT

Crystalline 2,4-dihydroxybenzylidene-4-aminoantipyrine ( $\text{HL} \cdot 0.5\text{H}_2\text{O}$ , **Ia**) undergoes desolvation followed by phase transformation in the solid state upon heating. The  $\text{UO}_2(\text{VI})$  complex of this ligand [ $\text{UO}_2\text{L}(\text{OOCCH}_3) \cdot 2\text{H}_2\text{O}$ , **IIa**] shows thermochromism in the solid state. This thermochromism has been attributed to desolvation accompanied by a phase change. These were studied using differential thermal analysis, thermogravimetric analysis, IR spectroscopy, X-ray powder diffraction and electrical conductivity. The energy of activation  $E_a$  of the desolvation processes and the reaction orders were evaluated.

### INTRODUCTION

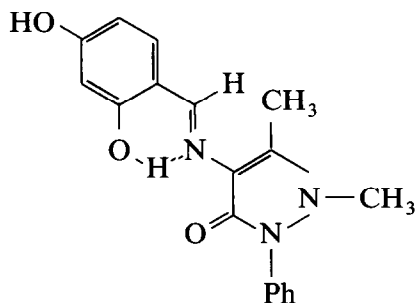
Antipyrine and its derivatives have different pharmaceutical activities [1,2] including antipyretic, analgesic and antihistaminic activity. Antipyrines have also been used as analytical reagents in the estimation of some metal ions [3–6]. A number of metal complexes of some Schiff-base derivatives of antipyrine have recently been prepared and characterised [7–10]. More recently the thermochromism in some  $\text{Ni}^{\text{II}}$ ,  $\text{V}^{\text{III}}$  and  $\text{Co}^{\text{II}}$  complexes has been studied [11–13]. This paper reports the thermal behaviour of crystalline 2,4-dihydroxybenzylidene-4-aminoantipyrine and its  $\text{UO}_2(\text{VI})$  complex using DTA, TG, X-ray powder diffraction, IR and electrical conductivity measurements. The kinetic parameters of the thermal reactions are also evaluated.

### EXPERIMENTAL

2,4-Dihydroxybenzylidene-4-aminoantipyrine ( $\text{HL} \cdot 0.5\text{H}_2\text{O}$ , **Ia**) was prepared according to known procedures [7]. The ligand was purified by

\* Author to whom correspondence should be addressed.

repeated recrystallisation from ethanol. The structure formula of the ligand is shown below.



The  $\text{UO}_2(\text{VI})$  complex of this ligand was prepared and characterised as described elsewhere [10]. The chemical formula of this complex is  $\text{UO}_2\text{L}(\text{OOCCH}_3) \cdot 2\text{H}_2\text{O}$ . Differential thermal analysis (DTA) was carried out at a heating rate of  $10^\circ\text{C min}^{-1}$  using a Shimadzu XD-30 thermal analyser. Thermogravimetric analysis (TG) was carried out using a DT-30 B thermal analyser (Shimadzu, Kyoto, Japan). IR spectra were measured as KBr discs or in Nujol mull using a Perkin-Elmer 598 ( $4000\text{--}200\text{ cm}^{-1}$ ) spectrophotometer. X-ray powder diffraction was measured using a Shimadzu XD-3 diffractometer and applying  $\text{Cu K}\alpha$  radiation. The electrical conductivity measurements were carried out on pressed discs ( $700\text{ kg cm}^{-2}$ ) of the ligand and its complex (diameter 13 mm and thickness 2–3 mm) using a Super Megohmmeter (model RM 170) electrometer, as described elsewhere [14].

## RESULTS AND DISCUSSION

The DTA curve of crystalline **Ia** (Fig. 1) shows three endothermic peaks at  $60^\circ\text{C}$ ,  $106^\circ\text{C}$  and  $229^\circ\text{C}$ . The TG, IR spectra and X-ray powder diffraction measurements show that these peaks are attributable to desolvation, phase change and melting, respectively. The TG measurement shows a weight loss corresponding to 0.5 mol of water. This is in good agreement with the elemental analysis of the crystalline ligand. The desolvation reaction and the phase change are irreversible, as indicated by the disappearance of their DTA peaks in the DTA curves of the samples heated (Fig. 1) at  $60^\circ\text{C}$  and  $106^\circ\text{C}$  for about an hour, respectively.

Figure 2 shows that the IR spectra of both the solvated (**Ia**) and desolvated (**Ib**) species are very similar. This indicates that no structural changes accompany the desolvation process. However, the spectrum of the sample heated at  $106^\circ\text{C}$ , compared to that of **Ia**, shows minor differences in

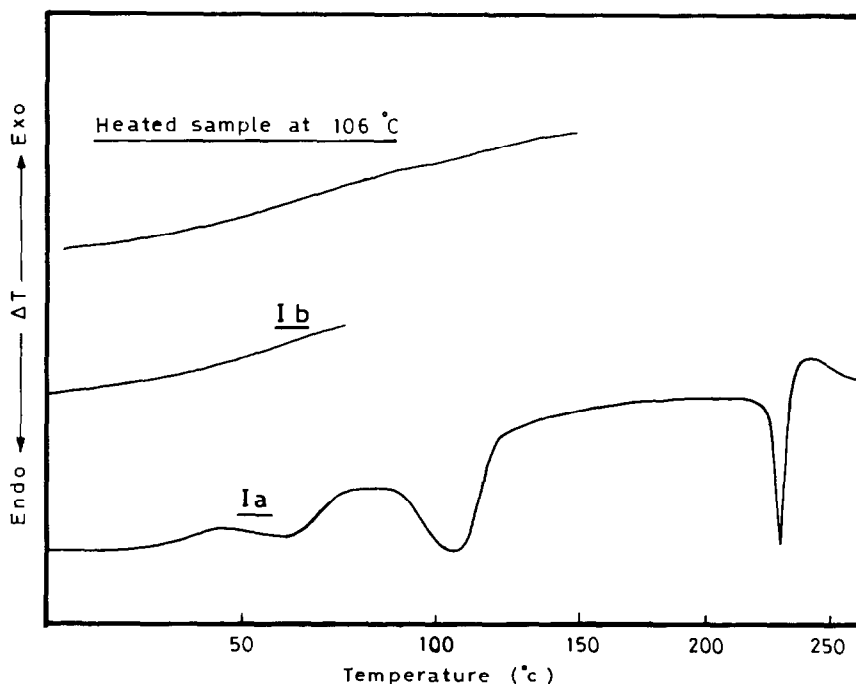


Fig. 1. DTA curves for the solvated (**Ia**) and desolvated (**Ib**) samples and that heated at  $106^{\circ}\text{C}$ .

the shape, intensity and position of some bands especially the out-of-plane CH deformation at  $850\text{ cm}^{-1}$ , the in-plane CH bending mode near  $1320\text{ cm}^{-1}$ , the O-H $\cdots$ N stretching mode at  $3150\text{ cm}^{-1}$  and the stretching mode of the *p*-OH group at  $3470\text{ cm}^{-1}$ . These spectroscopic changes may be attributable to changes in the molecular packing.

The above assignment of the DTA peaks of **Ia** was also confirmed by the X-ray powder diffraction patterns of **Ia**, **Ib** and of a sample heated at  $106^{\circ}\text{C}$ . Figure 3 shows that the patterns of both solvated (**Ia**) and desolvated (**Ib**) products do not show any significant changes. This indicates that the desolvation process is not accompanied by any structural changes. This is also evidence for the weak interaction of water, i.e. water plays little or no role in holding the crystal together and occupies the crystal voids [15]. However, the patterns of the sample heated at  $106^{\circ}\text{C}$  and the solvated (**Ia**) species are different. This difference is attributable to thermally induced molecular rearrangements which change the molecular interactions and the packing in the lattice.

The  $\text{UO}_2(\text{VI})$  complex of **Ia** has the chemical formula  $\text{UO}_2\text{L}(\text{OOCCH}_3) \cdot 2\text{H}_2\text{O}$  in which L is coordinated to the metal ion as a monobasic tridentate ligand through the phenolic oxygen atom, the imine nitrogen and the

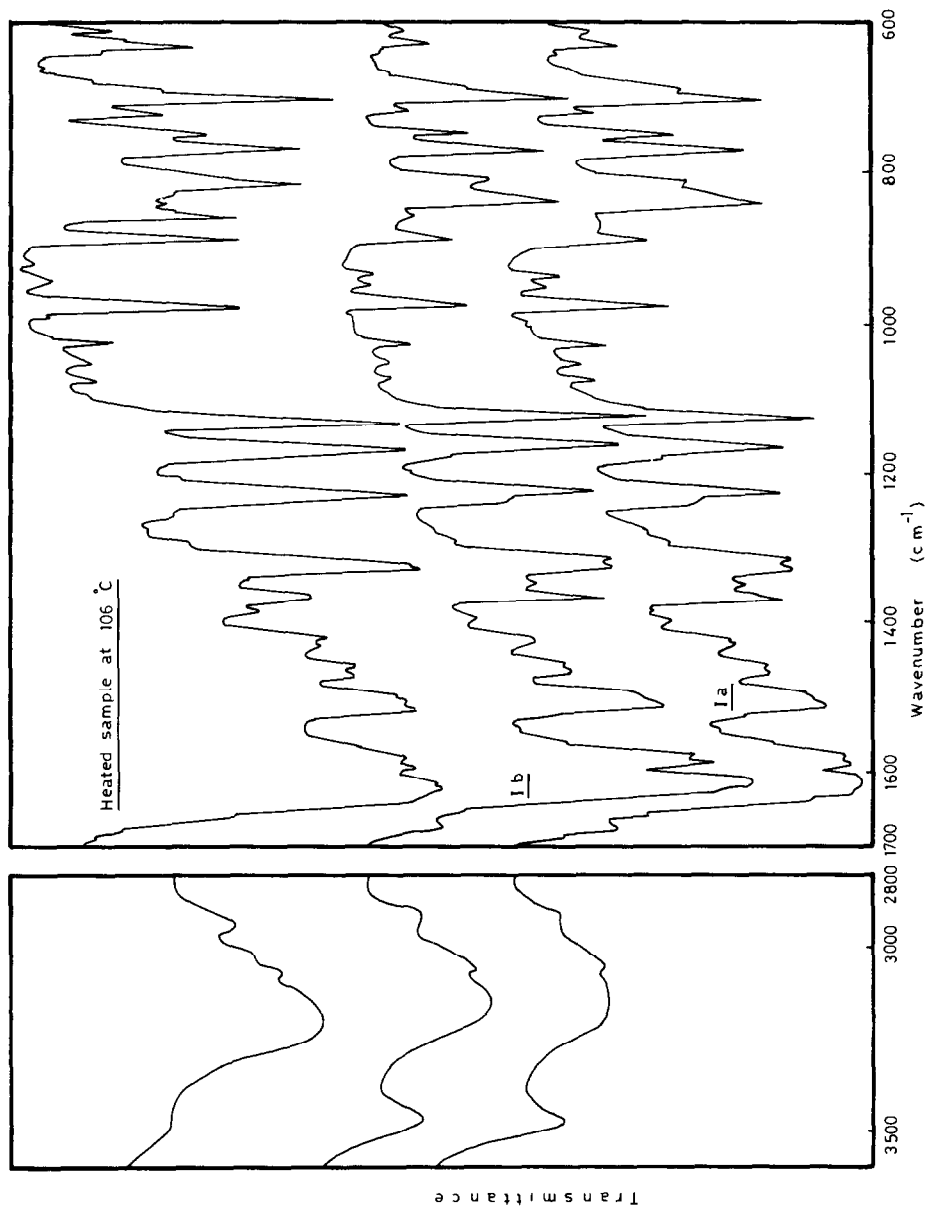


Fig. 2. IR spectra of Ia, Ib and the sample heated at 106 °C.

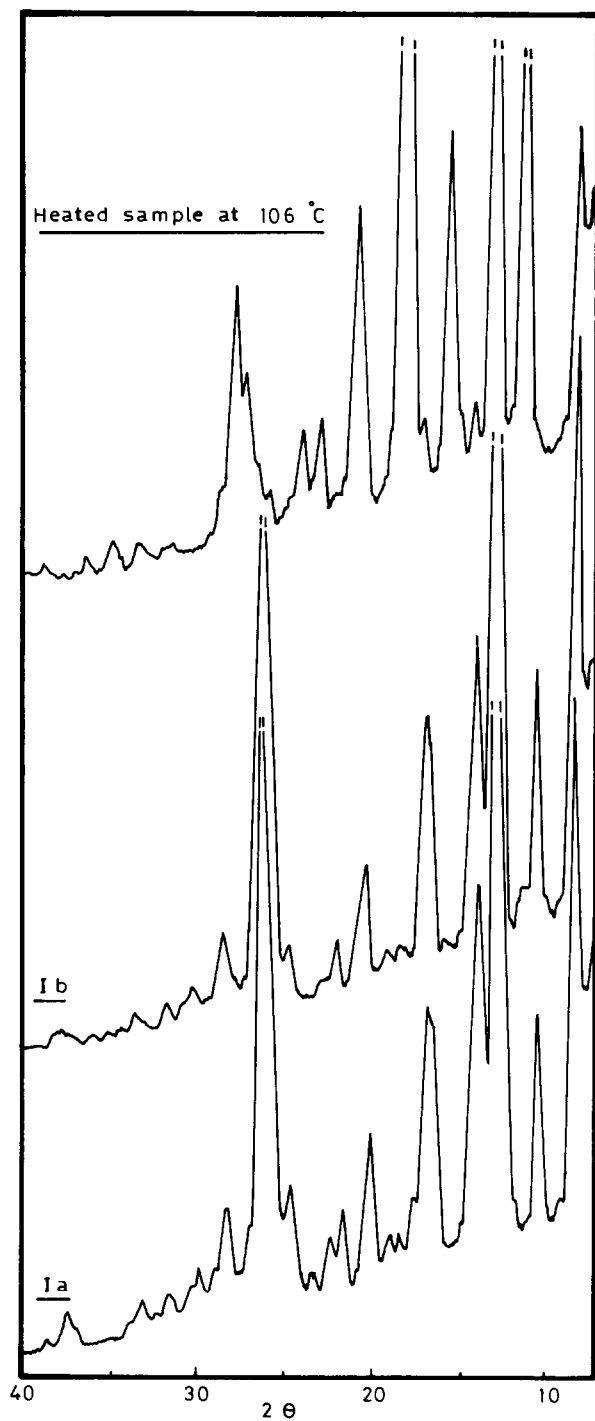


Fig. 3. X-ray powder diffraction patterns of **Ia**, **Ib**, and a sample heated at 106°C.

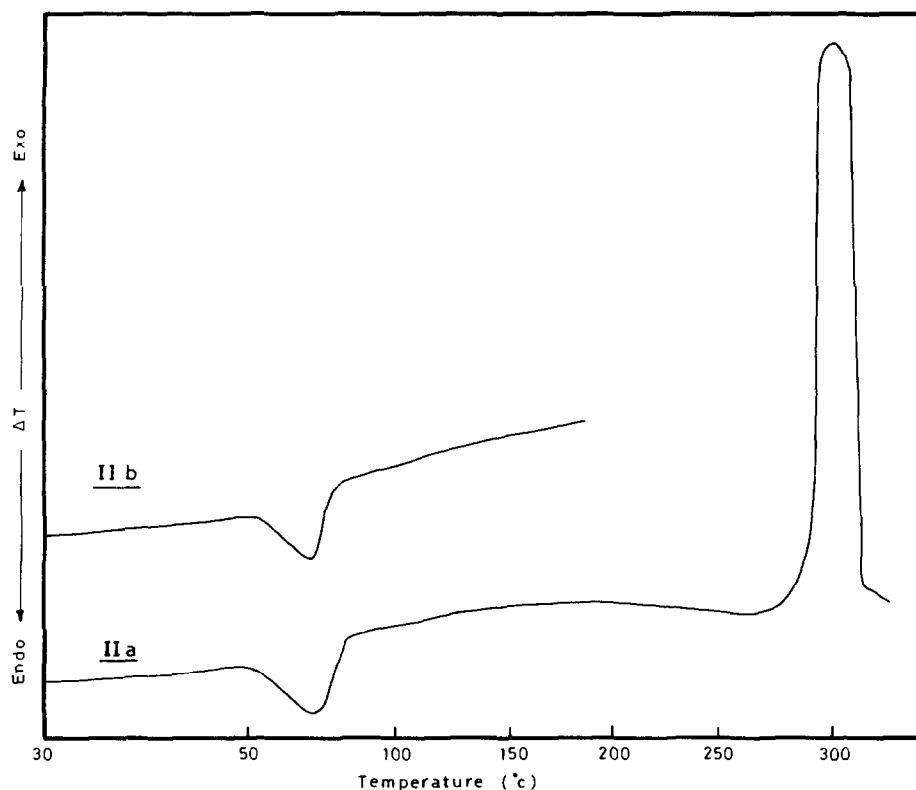


Fig. 4. DTA curves for **IIa** and **IIb**.

carbonyl oxygen of the pyrazolone ring. The acetate group acts as a bidentate ligand.

The complex **IIa** is brown and changes to red on heating to approximately 65°C. The corresponding red complex is referred to hereafter as **IIb**. The change in colour is reversible and the red form rapidly changes to brown again on standing in air at room temperature for about 5 min. This reversibility can be delayed for about 2 h if the red form is kept under paraffin oil. The TG measurement shows a weight loss corresponding to two molecules of water. This is in good agreement with the structure of the complex. The DTA curve of the brown complex **IIa** (Fig. 4) shows an endothermic peak at 65°C along with an exothermic peak at 300°C. These peaks have been assigned by other analytical and spectral measurements to the desolvation of **IIa** and the decomposition of the material, respectively. The temperature range of the thermochromism coincides with the DTA endothermic peak as shown in Fig. 4, indicating that the thermochromism can be attributed to the desolvation of **IIa** → **IIb**. Again the reversibility of the desolvation reaction was also confirmed by the occurrence of the endothermic peak in the DTA curve of **IIb**.

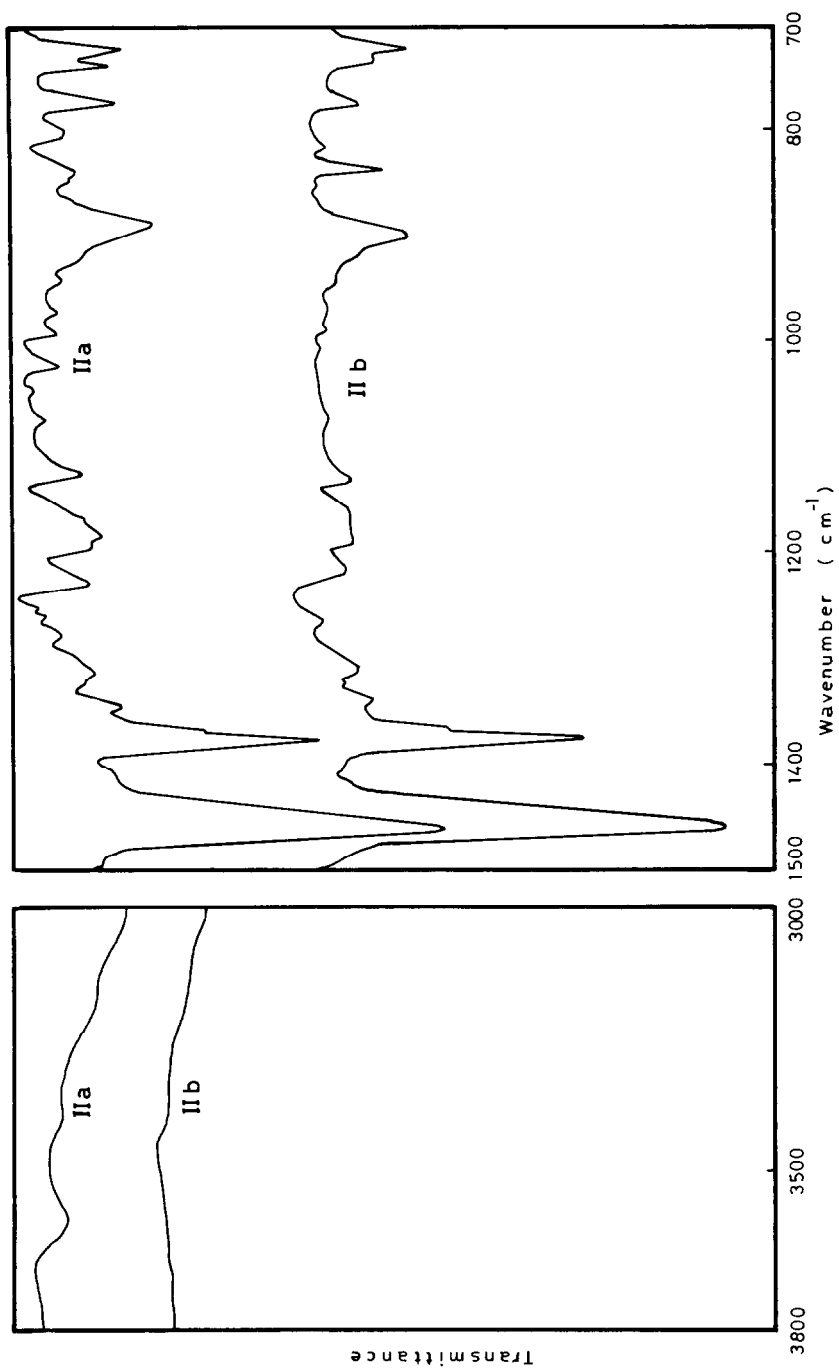


Fig. 5. IR spectra of IIa and IIb.

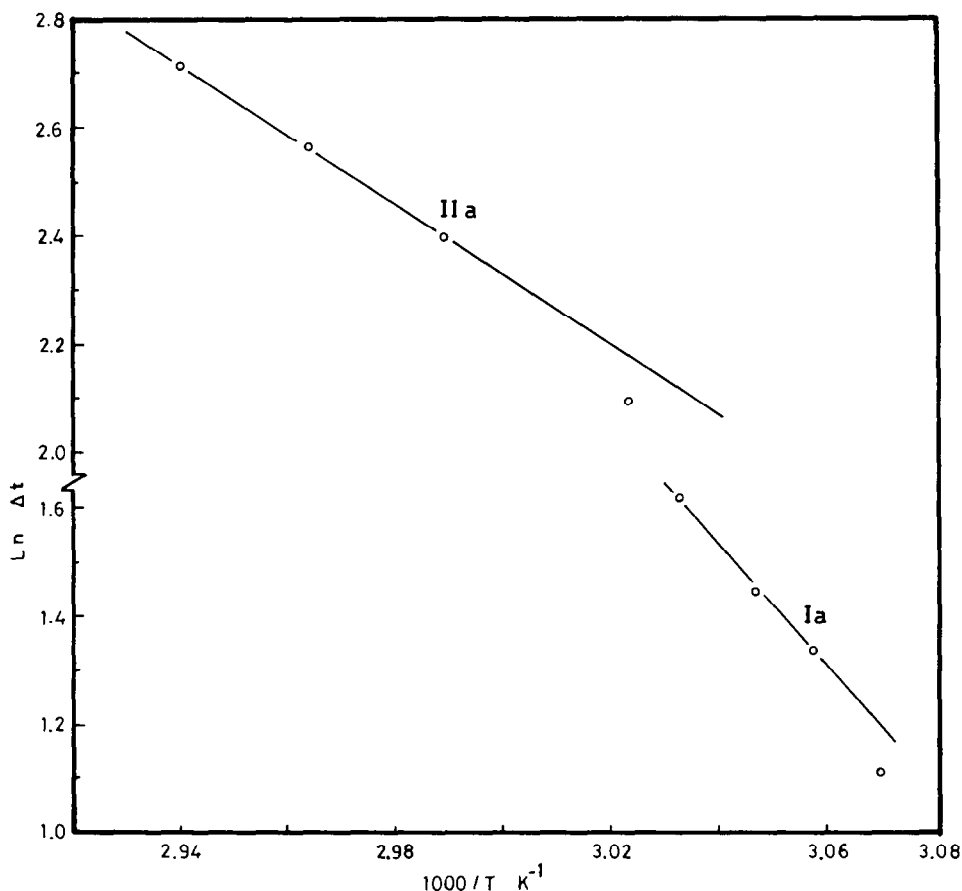


Fig. 6. Plots constructed from DTA curves of **Ia** and **IIa**.

The IR spectra of the brown (**IIa**) and red (**IIIb**) complexes in Nujol mull (Fig. 5) show minor differences in the shape, intensity and position of some bands. The out-of-plane CH deformation band near  $840\text{ cm}^{-1}$  is sharp and split into two bands in the spectrum of **IIIb**. Also, the in-plane CH bending mode near  $1225\text{ cm}^{-1}$  is broad and shifted to a lower frequency. The antisymmetric  $\nu_3(\text{O-U-O})$  band at  $885\text{ cm}^{-1}$  was shifted to a higher frequency in the spectrum of **IIIb**. These spectral changes may be due to changes in packing in the lattice (phase change). This also provides evidence for the strong interaction of water molecules, i.e. water plays a major role in holding the crystal together [15]. The desolvation of **IIa** was also confirmed by the disappearance of the  $\nu(\text{O-H})$  band of water at  $3580\text{ cm}^{-1}$  from the spectrum of **IIIb**. The rapid reversibility of the desolvation process precluded X-ray powder diffraction measurements.

The energies of activation ( $E_a$ ) of the desolvation reactions of both **Ia** and **IIa** were calculated from the DTA curves (Fig. 6) using the method of Piloyan et al. [16]. The  $E_a$  values of **Ia** and **IIa** are  $89.12$  and  $53.56\text{ kJ mol}^{-1}$ ,



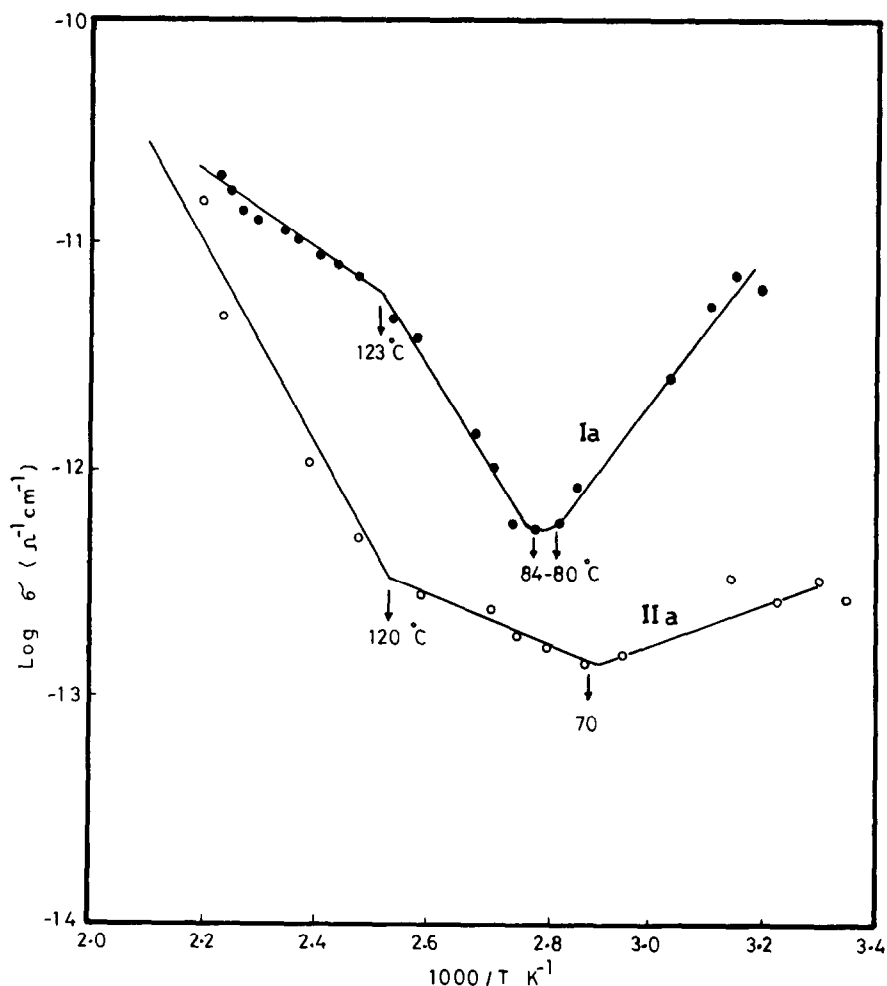


Fig. 7. Temperature dependence of the electrical conductivity of **Ia** and **IIa**.

respectively. The orders of the desolvation reactions were also evaluated using Reich's empirical relation [17]. The calculated values of  $n$  are 1.26 and 0.98 for **Ia** and **IIa** respectively, indicating that the desolvation reactions are first order.

Figure 7 shows the variation in the logarithmic electrical conductivity ( $\log \sigma$ ) versus the reciprocal absolute temperature ( $1000/T$ ,  $\text{K}^{-1}$ ) for the ligand (**Ia**) and its  $\text{UO}_2(\text{VI})$  complex (**IIa**). It can be shown that both **Ia** and **IIa** show metallic conduction in the temperature range 25–84°C, then semiconducting behaviour at higher temperatures with phase changes at 123 and 120°C, respectively. The metallic behaviour can be attributed to the loss of water molecules from the ligand and its complex. It is worth noting that the temperatures of the desolvation process obtained from IR, DTA and TG measurements of **Ia** and **IIa** are in accordance with metallic–semi-

conduction transitions. The discontinuity in the semiconducting region can be ascribed to a molecular rearrangement or to crystallographic transitions [18]. The activation energies,  $\Delta E_1$  and  $\Delta E_2$ , are deduced from the relationship  $\sigma = \sigma^\circ \exp(-\Delta E/KT)$ . These are 0.899 and 0.399, and 0.248 and 0.825 eV for both the ligand and its metal complex respectively.

## REFERENCES

- 1 P.J. Meffin, R.L. Williams, T.F. Blaschke and M. Rowland, *J. Pharm. Sci.*, 66 (1977) 135.
- 2 E.V. Schmidt, T.P. Priskchep and N.A. Chernova, *Izv. Tomsk. Politekh. Inst.*, (1975) 156; M.M. Shoukry, A. Kh. Ghoneim, E.M. Shoukry and M.H. El-Nagdi, *Synth. React. Inorg. Met. Org. Chem.*, 12 (1982) 815.
- 3 N.L. Olenovich and L.I. Koval Chuk, *Zh. Anal. Khim.*, 28 (1975) 2162.
- 4 Sh.T. Talipov, A.T. Tashkhodzhaev, L.E. Zel'tser and Kh. Khilkmatov, *Izv. Vyssh. Uchebn. Zaved. Khim. Tekhnol.*, 15 (1975) 1109.
- 5 V.V. Savant, P.P. Ramamurthy and C.C. Patel, *J. Less-Common Met.*, 22 (1970) 479.
- 6 B. Janik and S. Sawicki, *Mikrochim. Acta*, (1970) 1050.
- 7 T. Radhakrishnan, P.T. Joseph and C.P. Prabhakaran, *J. Inorg. Nucl. Chem.*, 38 (1976) 2217.
- 8 B. Kuncheria and P. Indrasenan, *J. Polyhedron*, 7 (1988) 143.
- 9 A.M. Donia and F.A. El-Saied, *J. Polyhedron*, 7 (1988) 2149.
- 10 F.A. El-Saied, *J. Inorg. Chim. Acta*, 165 (1989) 147.
- 11 A.M. Donia and E.M. Ebeid, *Thermochim. Acta*, 131 (1988) 1.
- 12 A.M. Donia, S.A. Amer and M.M. Ayad, *Thermochim. Acta*, 137 (1989) 189.
- 13 A.M. Donia and M.A. El-Rayes, *Thermochim. Acta*, 147 (1989) 65.
- 14 M.M. Ayad, M. Gaber and S.A. Azim, *Thermochim. Acta*, 147 (1989) 57.
- 15 S.R. Byran, *Solid State Chemistry of Drugs*, Academic Press, New York, London, 1982.
- 16 G.O. Piloyan, I.D. Raybchikov and O.S. Novikova, *Nature*, 5067 (1966) 1229.
- 17 T. Reich, *J. Inorg. Nucl. Chem.*, 28 (1966) 1329.
- 18 F. Gutmann and A. Metschey, *J. Chem. Phys.*, 36 (1962) 2355.